Criteria for Homogeneous Flash Boiling Atomization: An Experimental Approach

Yahav Moshkovich*[1], Yeshayahou Levy[1], Eran Sher[1]

[1]Faculty of Aerospace Engineering, Technion - Israel Institute of Technology, Haifa, Israel

*Corresponding author: yahavmoshko@gmail.com

Abstract

When liquid at a high pressure is driven out through an orifice to below its saturation pressure, flash-boiling of the homogeneous nucleation type may occur such that it results high quality liquid atomization. This is one of the most effective means of generating a fine and narrow-dispersed spray. The occurrence of flash boiling atomization involves kinetic stability problems that are characterized by two criteria which include a high enough initial liquid temperature and a high enough pressure drop rate. In this work, we analyzed the required high initial liquid temperature, and we used TSI's Phase Doppler Particle Analyzer (PDPA), to study the effect of the initial temperature and pressure on the spray cloud spatial pattern, droplets size distribution and velocity profile, on homogeneous flash boiling atomization system

Keywords

Flash boiling atomization, Homogeneous nucleation and Spray structure and Droplet size distribution.

Introduction

When a liquid at a high pressure is allowed to flow through an orifice towards a low ambient pressure which is below its saturation pressure, bubbles' nucleation is likely to occur. In fuel atomization systems, the nucleation is followed by bubbles' growth, leading to bubbles' burst and consequently to liquid jet atomization. Depending on the liquid initial temperature, its critical temperature, the ambient pressure and the rate of pressure drop, two major types of nucleation's may occur; nucleation at the liquid/solid interface (heterogeneous nucleation), and nucleation at the liquid bulk (homogeneous nucleation) [1,2].

As compared to heterogeneous nucleation, homogeneous nucleation results in a much finer and more uniform spray. In general, higher nucleation rate (more intense) results in a finer spray [3–9]. The most intensive nucleation occurs when the liquid reaches the kinetic stability limit (the explosion nucleation limit) (point C' in Fig. 1). At this point molecular fluctuations lead to spontaneous (homogeneous) nucleation with enormous large number of nucleation sites per unit volume. Previous experimental observations revealed that the liquid may reach the kinetic stability conditions only if the initial temperature of the liquid is above 90% of its critical value, and also, the pressure drop rate is above a critical value [10–14]. In this work, we analyze these observations, and implement a logically based explanation for the minimum initial temperature that is necessary to reach the kinetic stability limit (point C' in Fig. 1).
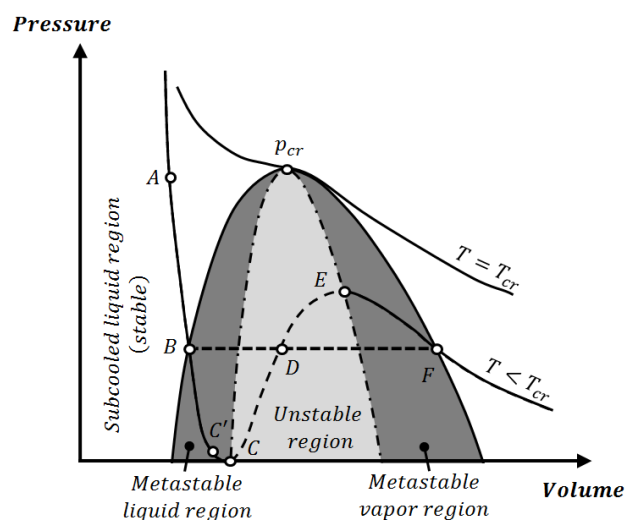
Figure 1. Example Pressure-volume diagram for a pure substance.

Evaluation of the liquid minimum initial temperature

We assume that the rate of the pressure drop is high enough such as the total number of the nuclei that are generated along the depressurized process is low and the time allowed for the nuclei' to grow is extremely short (line A-C' in Fig. 1). Under these conditions, the liquid may be assumed to undergo an isothermal process. We note that the temperature drop of the liquid is estimated to be only around $1K$ [15,16], and thus the assumption of isothermal expansion is fairly good.

For an isothermal process, it is clear from Fig. 1 that in order to reach the kinetic stability limit (point C'), a relatively high initial liquid temperature is required. Further we assume that the pressure at the kinetic stability limit is fairly close to the minimum spinodal pressure (i.e., to the thermodynamic stability limit – point C in Fig. 1). It can be shown that the pressure standard deviation of the pressure fluctuations far from the critical conditions, is in the order of $1/\sqrt{N}$, where N is the number of particles per unit volume. The difference between these two points, is thus insignificant.

The lowest initial temperature is thus the lowest possible isotherm for which $[(dp_r/dv_r)_T]_{at\ p_r=0} = 0$ (point C in Fig. 1 at $p_r = 0$). In order to find this lowest isotherm let's consider a general EOS of the form of [17]:

$$p_r = \frac{aT_r}{v_r - b} - \frac{c}{T_r^\lambda v_r (v_r + d)} \tag{1}$$

Where, p_r, T_r, and v_r are the relative pressure, temperature and volume with respect to their critical values, respectively. The constants a, b, c, d and λ, are different for each particular EOS model.

For the conditions $(p_r)_{T_r} = 0$ and $(\partial p_r/\partial v_r)_{T_r} = 0$ (denotes the minimum value of along an isotherm), the general EOS yields two algebraic equations that may be solved to yield the minimum allowable temperature. The values of the constants $a, b,$ and c may easily be found by using the properties of the substance at the critical point, i.e., $[(\partial p_r/\partial v_r)_T]_{cr} = 0$ and $[(\partial^2 p_r/\partial v_r^2)_T]_{cr} = 0$. For the Redlich-Kwong EOS, $a = 3, b = 0.2599, c = 2.8473, d = b$ and $\lambda = 0.5$ which results $v_r = 0.627, T_r = 0.895$.

Figure 2 shows some results of the minimum spinodal pressure along an isotherm vs. the isotherm temperature. Noted is the superiority of the Redlich-Kwong EOS which was found to fit best the observed isotherms inside the saturation region for a large number of relevant pure substances [15,17]. In particular noted in Fig. 2 are the intersections of the three EOS's with the horizontal axis ($p_r = 0$). The temperature in this intersection denotes the minimum initial temperature that still allows to reach the thermodynamic stability conditions (point C in Fig. 1). The figure presents some experimental results of several different liquids together with the results of the present proposed concept while using three different well established equations of state (EOS), each at a time [2,18]. The results of the two other EOS's are depicted in the figure for reference. The remarkable fitting between our predictions with the Redlich-Kwong EOS and the experimental results seems to fairly support our proposed concept [15] as above.
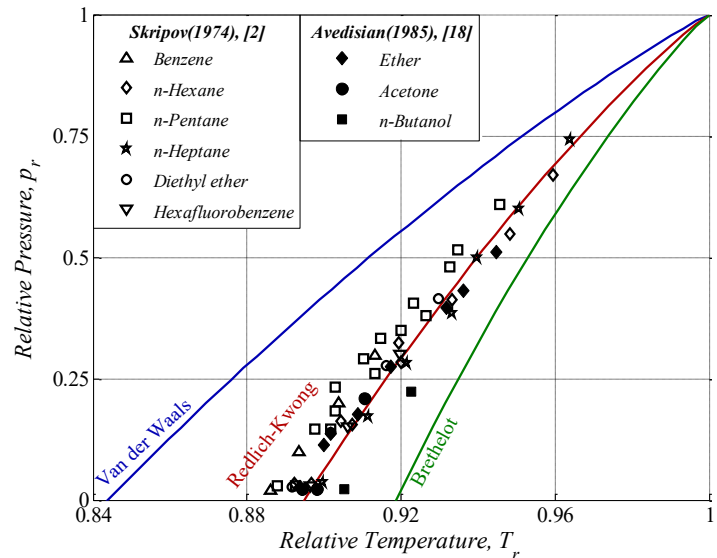
Figure 2. Some results of the minimum spinodal pressure along an isotherm (the thermodynamic stability limit, point C in Fig. 1) vs. the isotherm temperature and experimental results from Skripov (1974) [2] in hollow symbols and Avedisian (1984) [18] in filled symbols. Noted is the liquid minimum initial temperature that enable to reach the thermodynamic stability conditions (T_r at $p_r = 0$).

Experimental setup

The experimental system consists of a spray generator that used a rapid depressurization process, and a measuring system to measure the spray characteristics [7]. The main objective is to study the evolution of the spray characteristics of a spray that is generated from a one-component fluid that flows through a single-orifice and undergoes homogeneous nucleation prior to its disintegration. For the sake of simplicity, Chlorodifluoromethane, CHClF2 (R-22), has been selected for its suitable properties: its relatively low critical temperature and relatively low saturation pressure at 89% of the critical temperature significantly simplified the spray generation system; its safety properties (health, flammability and reactivity) also simplified the system; and its optical properties (opacity and refractive index) are suitable for using the Phase Doppler Particle Analyzer (PDPA) (Table 1).

In the present set of experiments, the effect of initial liquid pressure and temperature on the spray cloud spatial pattern, droplets size distribution and velocity profile, were examined. The initial temperature range was selected such as to examine the initial temperature criterion for a homogeneous nucleation, around $332\,K$ ($56°C$) that is 90% of the critical temperature of CHClF2.

Table 1. R-22 properties at $56°C$ ($0.89T_{cr}$).

Property	Value
Critical temperature, K	369.3
Critical pressure, MPa	4.99
Saturation pressure, MPa	2.39
Surface tension, N/m	0.004
Refractive index	1.22

Spraying system

The schematic of the spray generator system is illustrated in Fig. 3 [7]. The liquid is pressurized in its original container to its saturation pressure that corresponds to the ambient temperature. A well-controlled amount of R-22 is delivered to the pressure tank where it is cooled down and condensed. Next, the original container is closed and the pressure tank is heated to ambient. Compressed Nitrogen is then allowed to flow into the pressure tank to pressurize the R-22 to the desirable level. The R-22 liquid is allowed to discharge through a fine dense filter ($15\mu m$ mesh) and then through a simple plane atomizer (Fig. 4) while its path is heated to maintain the desirable temperature.
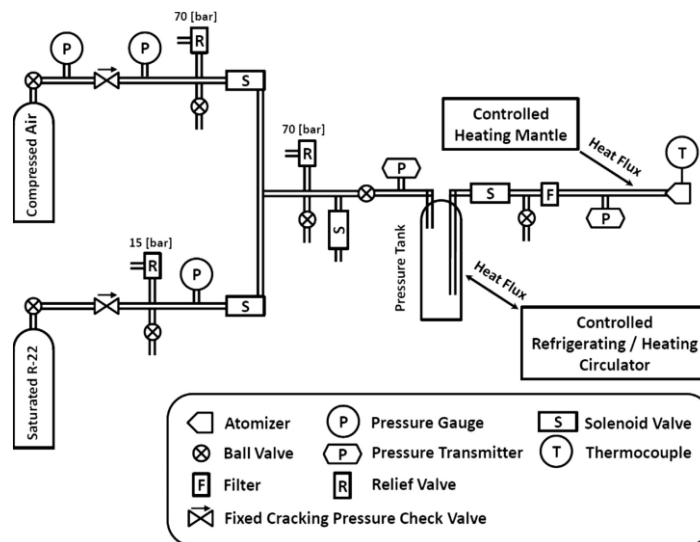
Figure 3. The spray generating system [7].

(a) *(b)*
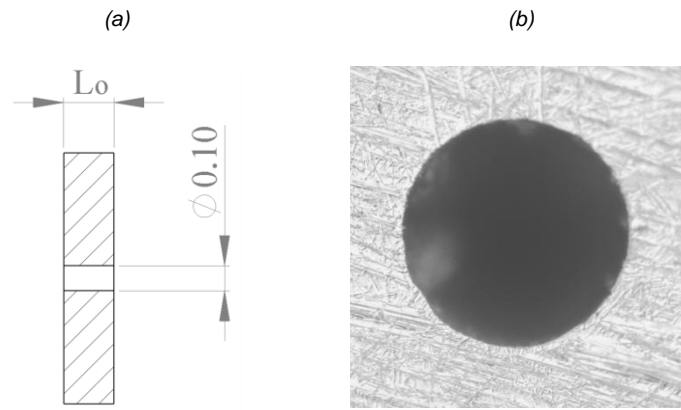
Figure 4. a. Orifice dimensions [mm]. b. Orifice photo taken by lens x50, microscope.

Method

We used TSI's Phase Doppler Particle Analyzer (PDPA) to characterize the spray. The PDPA measuring system (Fig. 3) generates a control volume in the intersection region of two monochromatic and coherent focused laser beams. The liquid droplets that passes through that control volume scatter light with modulated intensity. A receiving optics focuses a portion of the scattered light into a multi detector receiver that convert the light into electric signals for further processing. After introducing the R-22 refractive index to the system's software, the signals received in the detectors may be used to analyze the droplets' diameter and velocity. We also used a controlled 3D positioning system to measure these droplets characteristics at different accurate and specific position relative to the orifice position and the symmetric axis of the spray.

The measuring sequence for each measuring point included seven steps: positioning the orifice in a desirable point to measure parameters at a specific distance H from the orifice; scanning the spray crosswise using the PDPA to detect the symmetric axis of the spray; positioning the system to measure parameters at a specific distance R from the symmetric axis; adjusting the spray formation system till a desirable initial temperature and pressure is achieved; waiting for the spray to stabilized; sampling 20,000 droplets using the PDPA measuring system; and analyzing the droplets' characteristics using TSI's FLOWSIZER™ system software.

Sampling of 20,000 droplets per measuring point allowed us using statistic tools to analyze the spray characteristics such as the velocity histograms and its mean values, mean diameter and Sauter Mean Diameter (SMD).

The mean velocity was calculated from $\bar{V} = 1/n_v \sum_{i=1}^{n_v} V_i$ where V_i is the velocity of droplet i, and n_v is the total number of velocity valid counted droplets.

The diameter statistics includes several types of mean diameters, a generalized mean diameter can be defined [19], cited by Lefebvre [20] as $D_{pq} = \left(\sum_{j=1}^{n_d} D_j^p / \sum_{j=1}^{n_d} D_j^q\right)^{1/p-q}$ where p and q designate the index of interest. Here D_j is the diameter of droplet j, and n_d is the total number of diameter valid counted droplets.

Two relevant mean diameters are the arithmetic mean diameter, $D_{10} = 1/n_d \sum_{j=1}^{n_d} D_j$, and the mass transfer index - the Sauter Mean Diameter (SMD), $D_{32} = \sum_{j=1}^{n_d} D_j^3 / \sum_{j=1}^{n_d} D_j^2$.

Measurements uncertainty

According to the PDPA manual, in a well aligned system, the typical velocity measurement accuracy of each droplet is about 1%, and about 5% for the droplet diameter. Since at each measuring point we sampled 20,000 droplets, considering an accuracy of about 1% for the mean velocity and 5% for the mean diameter is fairly reasonable. The pressure transmitter that was used to measure the injecting pressure depicts an accuracy of 0.25% and nonlinearity of 0.5%. Around the measuring points $(4 - 5\ MPa)$, the typical inaccuracy is about $0.01\ MPa$. The atomizer and the pipeline were temperature controlled using a heating mantle. The accuracy of the K thermocouples is $\pm 2K$.

Results and discussion

We sampled 100 points under a fairly wide range of initial temperatures and pressures. For each point we recorded about 20,000 validated signals for the size and velocity of the droplets. Generally, we observed a clear change in the mean velocity and arithmetic and Sauter mean diameters (D_{10} and D_{32}) of the droplets, around the temperature criterion.

Mean diameter

Figure 5 shows the same trend for the dependence of the average diameter D_{10} on the temperature. At low temperatures, an average diameter change with temperature of about $-0.2 \mu m/°C$ (reduction of diameter with increasing temperature). At a certain temperature, within a range of $55 < T < 58 °C$ ($T_r = 0.89$), there is a sharp increase in diameter and above this area there is no clear behavior. This may Indicate a change between different nucleation regimes, in accordance with the criteria presented for obtaining homogenous flash spray. Note that the smallest average droplet size is obtained at the transition temperature between the nucleation regimes.

For all the sampled points, we noticed a Rosin-Rammler droplet size distribution. The effect of the temperature on the diameter cumulative distribution function is shown in Fig. 6.
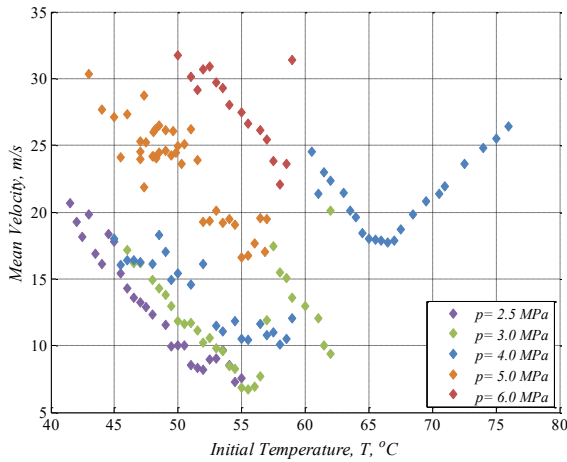
Figure 5. Mean diameter (D_{10}) vs. temperature at the centerline $H = 40mm$ downstream and different initial pressure.
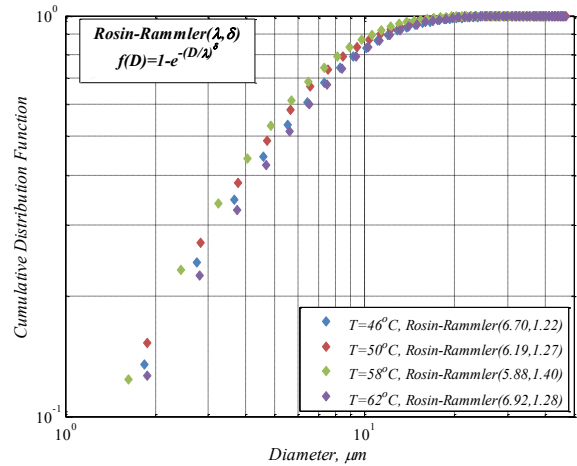
Figure 6. The effect of the temperature on the diameter cumulative distribution function at the centerline $H = 40mm$ downstream, at initial pressure $p = 4MPa$ and at different initial temperature. Here, $Rosin - Rammler(\lambda, \delta)$ denotes Rosin-Rammler diameter cumulative distribution function with representative diameter λ and spread of drop size δ.

Fig. 7 show the dependency of the Sauter mean diameters (D_{32}) on the temperature. Here, it shows that at low pressures, there is a similar behavior of the average diameter (Fig. 5), indicating a variation in SMD with temperature of about $-0.25 \mu m/°C$. In high pressures ($p = 5,6MPa$) a moderate decline is noted.
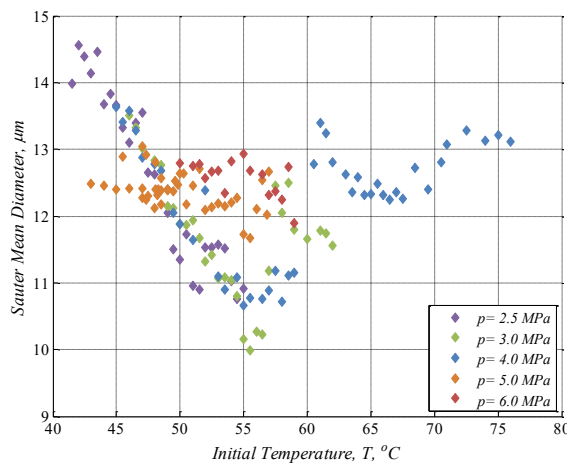
Figure 7. Sauter mean diameter (D_{32}) vs. temperature at the centerline $H = 40mm$ downstream and different initial pressure.

We would like to emphasize that in the present set of experiments, the initial pressure and temperature ranges were selected such as to ensure homogeneous nucleation at the atomizer orifice (see the experimental setup section).

Velocity

The effect of the initial temperature on the velocity profile is depicted in Fig. 8. Here, too, there is a similar behavior of the speed of the droplets. This may Indicates a change in the nucleation regime in the temperature zone of $T_r \approx 0.89$. In the low temperature range it can be seen that there is a relatively constant change of about $-1\ m/s$ per $°C$.

For all the sampled points, we noticed a Gaussian (normal) velocity distribution of the droplets. The effect of the temperature on the diameter velocity distribution is shown in Fig. 9.
It shows that in the low temperature range, in addition to the average decrease in velocity with temperature, the variance velocity distribution is smaller.
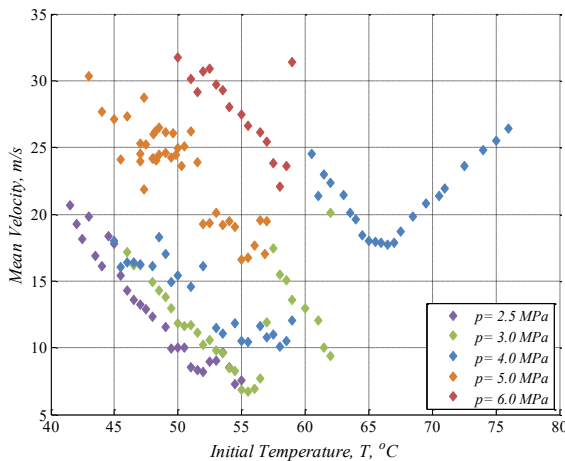
Figure 8. Mean centerline velocity at $H = 40mm$ downstream, vs. temperature and different initial pressure.
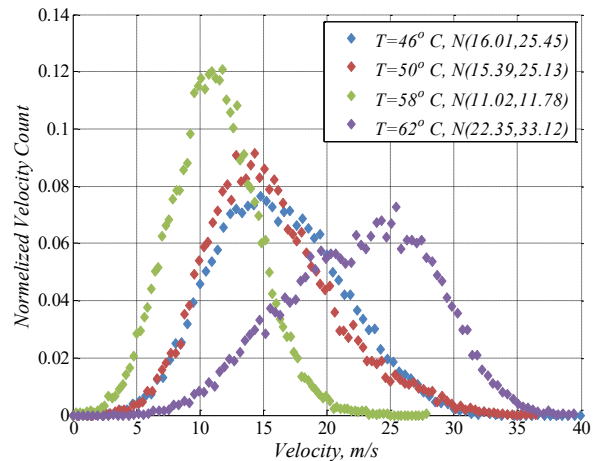
Figure 9. Velocity distribution at $H = 40mm$ downstream, at different initial temperature, for initial pressure $p = 4MPa$. Here, $N(\mu, \sigma^2)$ denotes Normal distribution with a mean diameter μ, and variance σ^2.

Conclusion

The first empirical criterion for flash-boiling fuel atomization of the homogeneous nucleation type has been developed from basic principles and hence is now fully explained. This criterion is essentially needed to reach the kinetic stability limit of a saturated liquid, and thus for obtaining a flash-boiling fuel atomization of the homogeneous nucleation type. The experimental results showed a clear border between heterogeneous to homogeneous nucleation regimes at temperature range about $0.88 < T_r < 0.9$.

Acknowledgments

References

[1] Sher, E., Bar-Kohany, T., and Rashkovan, A., 2008, "Flash-Boiling Atomization," Progress in Energy and Combustion Science, **34**(4), pp. 417–439.

[2] Skripov, V. P., 1974, *Metastable Liquids*, John Wiley & Sons LTD, New York.

[3] Park, B. S., and Lee, S. Y., 1994, "An Experimental Investigation of the Flash Atomization Mechanism," Atomization and Sprays, **4**(2), pp. 159–179.

[4] Zeigerson-Katz, M., and Sher, E., 1998, "Spray Formation by Flashing of a Binary Mixture: A Parametric Study," Atomization and Sprays, **8**(3), pp. 255–266.

[5] Rashkovan, A., and Sher, E., 2006, "Flow Pattern Observations of Gasoline Dissolved CO2 Inside an Injector," Atomization and Sprays, **16**(6), pp. 615–626.

[6] Zhifu, Z., Weitao, W., Bin, C., Guoxiang, W., and Liejin, G., 2012, "An Experimental Study on the Spray and Thermal Characteristics of R134a Two-Phase Flashing Spray," International Journal of Heat and Mass Transfer, **55**(15–16), pp. 4460–4468.

[7] Levy, M., Levy, Y., and Sher, E., 2014, "Spray Structure as Generated under Homogeneous Flash Boiling Nucleation Regime," Applied Thermal Engineering, **73**(1), pp. 416–423.

[8] Bar-Kohany, T., and Levy, M., 2016, "State of the Art Review of Flash-Boiling Atomization," Atomization and Sprays, **26**(12), pp. 1259–1305.

[9] Levy, M., Levy, Y., and Sher, E., 2016, "The Effect of the Propellant Mass Fraction in a Binary Mixture on the Spray Characteristics as Generated by Homogeneous Flash Boiling," Atomization and Sprays, **26**(12), pp. 1241–1257.

[10] Alamgir, M., and Lienhard, J. H., 1981, "Correlation of Pressure Undershoot During Hot-Water Depressurization," Journal of Heat Transfer, **103**(1), pp. 52–55.

[11] Abuaf, N., Jones, O., and Wu, B., 1983, "Critical Flashing Flows in Nozzles with Subcooled Inlet Conditions," Journal of Heat Transfer, **105**(2), pp. 379–383.

[12] Hutcherson, M. N., Henry, R. E., and Wollersheim, D. E., 1983, "Two-Phase Vessel Blowdown of an Initially Saturated Liquid—Part 2: Analytical," Journal of Heat Transfer, **105**(4), pp. 694–699.

[13] Elias, E., and Chambre, P., 1993, "Flashing Inception in Water During Rapid Decompression," Journal of Heat Transfer, **115**(1), pp. 231–238.

[14] Bartak, J., 1990, "A Study of the Rapid Depressurization of Hot Water and the Dynamics of Vapour Bubble Generation in Superheated Water," International Journal of Multiphase Flow, **16**(5), pp. 789–798.

[15] Moshkovich, Y., Levy, Y., and Sher, E., 2019, "Theoretical Criteria for Homogeneous Flash Boiling Atomization," Submitted.

[16] Sher, E., and Elata, C., 1977, "Spray Formation from Pressure Cans by Flashing," Industrial & Engineering Chemistry Process Design and Development, **16**(2), pp. 237–242.

[17] Carey, V. P., 2008, *Liquid Vapor Phase Change Phenomena: An Introduction to the Thermophysics of Vaporization and Condensation Processes in Heat Transfer Equipment*, Taylor & Francis Group, LLC.

[18] Avedisian, C. T., 1985, "The Homogeneous Nucleation Limits of Liquids," Journal of Physical and Chemical Reference Data, **14**(3), pp. 695–729.

[19] Mugele, R. A., and Evans, H. D., 1951, "Droplet Size Distribution in Sprays," Industrial & Engineering Chemistry, **43**(6).

[20] Lefebvre, A., 1988, *Atomization and Sprays*, CRC press, West Lafayette, Indiana.